

# Non-linear response of internal friction to tensile strain rate and frequency during plastic deformation of high-purity aluminium

J. X. ZHANG

*Department of Physics and Institute of Material Science, Zhongshan University, Guangzhou 510275, People's Republic of China*

J. K. L. LAI

*Department of Applied Science, City Polytechnic of Hong Kong, Tat Chee Avenue, Kowloon, Hong Kong*

The internal friction of high-purity aluminium during the process of plastic deformation was measured by a middle torsion pendulum on a modified tensile testing machine. The effects of tensile strain rate,  $\dot{\varepsilon}$ , in the range of  $0.73 \times 10^{-6}$  to  $50 \times 10^{-6} \text{ s}^{-1}$ , and frequency of internal friction measurement,  $f$ , in the range of 0.38 to 2.6 Hz were studied. The results showed a non-linear dependence of internal friction,  $Q^{-1}$ , on  $\dot{\varepsilon}$  and  $f^{-1}$ , or on  $\dot{\varepsilon}/\omega$  ( $\omega = 2\pi f$ ). The interrelationship between internal friction during the process of plastic deformation and dislocation motion, and the effect of non-linearity on the dynamic behaviour of dislocations are discussed.

## 1. Introduction

Low-frequency internal friction during the process of plastic deformation,  $Q^{-1}$ , and the technique of measurement using a middle torsion pendulum, were first reported by Maringer [1]. Subsequently, the  $Q^{-1}$  versus  $\varepsilon$  (tensile strain) curves for Al, Cu and Armco-Fe samples were determined by Kê *et al.* [2]. The fairly high values of  $Q^{-1}$  obtained by these investigators were attributed to the process of plastic deformation because they were observed only when  $\dot{\varepsilon} \neq 0$ . If  $\dot{\varepsilon}$  was changed from  $\dot{\varepsilon} \neq 0$  to  $\dot{\varepsilon} = 0$  suddenly (i.e. keeping  $\varepsilon$  constant), the  $Q^{-1}$  value dropped almost at once to a low background value [2]. Postnikov *et al.* [3] and Felthan and Newhan [4] investigated the effects of tensile strain rate  $\dot{\varepsilon}$  and angular frequency of internal friction measurement  $\omega$  on  $Q^{-1}$ , and reported linear dependence of  $Q^{-1}$  on  $\dot{\varepsilon}$  and on  $\omega^{-1}$ . More recently, the internal friction (IF) during the process of plastic deformation for Armco-Fe at values of strain within the yield plateau (i.e.  $Q^{-1}$  did not change with  $\varepsilon$ ) was studied by Zhang *et al.* [5], and a similar linear dependence was also observed.

Various theories have been presented in order to interpret these results. Postnikov *et al.* [3] and Felthan and Newhan [4] associated  $Q^{-1}$  with a thermal activation process and obtained a linear dependence of  $Q^{-1}$  on  $\dot{\varepsilon}$  and  $\omega^{-1}$  as  $Q^{-1} = \beta(\dot{\varepsilon}/\omega)$ , where  $\beta$  is a constant. Kê and Zhang [6] and Zhang [7] attributed  $Q^{-1}$  to the movement of dislocations. They obtained a similar expression but the parameter  $\beta$  was a function of stress  $\sigma$  instead of being a constant. They also obtained a dislocation dynamics expression relating the velocity  $V$  of moving dislocations to the effective stress.

The above theories were, however, based on the linear dependence of  $Q^{-1}$  on  $\dot{\varepsilon}$  and  $\omega^{-1}$  within a limited range of  $\dot{\varepsilon}$  and  $\omega$ . It is therefore important to extend this investigation by broadening the range of  $\dot{\varepsilon}$  and  $\omega$  studied. The areas of particular interest are the effects on  $Q^{-1}$  by varying  $\dot{\varepsilon}$  at low, but constant  $\omega$ , and by varying  $\omega$  at high, but constant  $\dot{\varepsilon}$ .

The present investigation aims to extend the range of previous studies for high-purity aluminium. The significance of the results obtained on the dynamic behaviour of dislocations is discussed.

## 2. Experimental procedure

The experimental technique used has been described previously [1, 2, 5]. The internal friction of high-purity aluminium during the process of plastic deformation was measured by a middle torsion pendulum on a modified tensile testing machine. The tensile strain rate  $\dot{\varepsilon}$  and frequency of measurement  $f$  used in the present investigation were  $\dot{\varepsilon}_1 = 0.73 \times 10^{-6} \text{ s}^{-1}$ ,  $\dot{\varepsilon}_2 = 1.53 \times 10^{-6} \text{ s}^{-1}$ ,  $\dot{\varepsilon}_3 = 2.94 \times 10^{-6} \text{ s}^{-1}$ ,  $\dot{\varepsilon}_4 = 6.35 \times 10^{-6} \text{ s}^{-1}$ ,  $\dot{\varepsilon}_5 = 12.1 \times 10^{-6} \text{ s}^{-1}$ ,  $\dot{\varepsilon}_6 = 25.3 \times 10^{-6} \text{ s}^{-1}$ ,  $\dot{\varepsilon}_7 = 50 \times 10^{-6} \text{ s}^{-1}$  and  $f_1 = 0.382 \text{ Hz}$ ,  $f_2 = 0.5 \text{ Hz}$ ,  $f_3 = 0.836 \text{ Hz}$ ,  $f_4 = 1.0 \text{ Hz}$ ,  $f_5 = 2.03 \text{ Hz}$ ,  $f_6 = 2.63 \text{ Hz}$ , respectively. All measurements were made at room temperature.

The wire-shaped specimen was prepared from a 99.9991% pure aluminium rod, about 8 mm in diameter and 50 mm in length, manufactured by the Light Co. (UK).

In order to avoid contamination by oil or other metals during specimen preparation, the bar was carefully hot-forged to about 4.5 mm diameter by hand

hammering at 200 to 250 °C, with repeated cleansing by dilute KOH solution before cold-drawing to 1.0 mm diameter. The last treatment was annealing at 400 °C for 0.5 h followed by furnace-cooling.

### 3. Theory

A common measure of the internal friction in the free decay mode, such as that in the middle pendulum used, is the logarithmic decrement  $\delta$ . When  $\delta/\pi$  or  $Q^{-1}$  is small, e.g. much less than 0.05, we have

$$Q^{-1} = \frac{1}{2\pi} \frac{\Delta W}{W} = \frac{\delta}{\pi} = \frac{1}{\pi n} \ln \left( \frac{A_0}{A_n} \right) \quad (1)$$

where  $W$  is the total energy of vibration,  $\Delta W/W$  the fractional energy loss per cycle, and  $A_0$  and  $A_n$  are the zeroth and  $n$ th amplitude of the vibration, respectively. When  $Q^{-1}$  or  $\delta/\pi$  is large, for example more than 0.05, Equation 1 is not accurate. The precise relationship between  $Q^{-1} = (1/2\pi) (\Delta W/W)$  and  $\delta/\pi$  depends on the mechanism of internal friction, but we can obtain a simple approximate relationship by the following calculations.

Using the expansion form of  $\delta = \ln(A_0/A_1) = \ln X$ , we have

$$\delta = \ln X = \frac{X-1}{X} + \frac{1}{2} \left( \frac{X-1}{X} \right)^2 + \dots \quad (2)$$

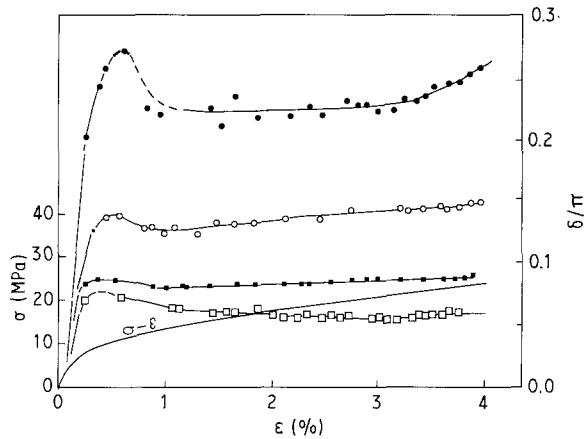


Figure 1 Effect of frequency on the  $\delta/\pi$  versus  $\epsilon$  curves at  $\dot{\epsilon} = 50 \times 10^{-6} \text{ s}^{-1}$ : (●)  $f_1 = 0.382 \text{ Hz}$ , (○)  $f_3 = 0.836 \text{ Hz}$ , (■)  $f_5 = 2.03 \text{ Hz}$ , (□)  $f_6 = 2.63 \text{ Hz}$ . The corresponding  $\sigma$  versus  $\epsilon$  curve is also shown.

for any value of  $\delta$ , and

$$Q^{-1} = \frac{1}{2\pi} \frac{\Delta W}{W} = \left( \frac{1}{2\pi} \right) \frac{A_0^2 - A_1^2}{A_0^2} = \left( \frac{1}{2\pi} \right) \frac{X^2 - 1}{X^2} = \eta(X) \left( \frac{\delta}{\pi} \right) \quad (3)$$

Thus we can relate  $\delta$  to  $Q^{-1}$ . The function  $\eta(X)$  depends on the number of terms incorporated in the expression for  $\delta$  in Equation 2. For example, if two terms are included, when  $\delta/\pi = 0.22$ ,  $X = 2$ ,  $\eta(X) = 0.6$  and  $Q^{-1} = 0.133$ ; when  $\delta/\pi = 0.03$ ,  $X = 1.1$ ,  $\eta(X) = 0.91$  and  $Q^{-1} = 0.028$ .

In this paper we define  $\delta/\pi$  as the apparent internal friction and use the true value of  $Q^{-1}$  calculated by Equation 3 for comparison with theoretical analysis.

### 4. Results

The influence of the frequency of measurement on  $\delta/\pi$  during the process of plastic deformation for high-purity Al at high strain rate ( $= 50 \times 10^{-6} \text{ s}^{-1}$ ) is shown in Fig. 1. The stress-strain ( $\sigma$  versus  $\epsilon$ ) curve is also shown in the figure. The frequencies of  $\delta/\pi$  measurement are 0.382 Hz ( $f_1$ ), 0.836 Hz ( $f_3$ ), 2.03 Hz ( $f_5$ ) and 2.63 Hz ( $f_6$ ), respectively. It is clear that  $\delta/\pi$  decreases with increasing frequency of measurement. The  $\delta/\pi$  versus  $\epsilon$  curve exhibits a maximum value after macro-yielding of the samples. For  $\epsilon > 1\%$ ,  $\delta/\pi$  shows a slightly increasing trend with increasing  $\epsilon$  at low frequencies. At the highest frequency  $f_6$ ,  $\delta/\pi$  exhibits a decreasing trend with increasing  $\epsilon$ .

The influence of frequency of measurement on  $\delta/\pi$  at low strain rate ( $\dot{\epsilon}_3 = 2.94 \times 10^{-6} \text{ s}^{-1}$ ) is shown in Fig. 2. Also shown in the same figure is the corresponding  $\sigma$  versus  $\epsilon$  curve. It is clear that  $\delta/\pi$  decreases with increasing frequency of measurement. In Fig. 2, one sample was tested at a constant frequency,  $f_4 (= 1.0 \text{ Hz})$ , throughout. The other sample was tested at three frequencies:  $f_1$  (0.382 Hz, when  $\epsilon < 3.6\%$ ),  $f_2$  (0.5 Hz, from  $\epsilon = 3.7\%$  to 4.1%) and  $f_4$  (1.0 Hz, when  $\epsilon > 4.1\%$ ). The maximum after yielding observed in Fig. 1 at high strain rate disappears in Fig. 2 at low strain rate. The  $\delta/\pi$  versus  $\epsilon$  curves are almost parallel to the abscissa after macro-yielding of the sample. The coincidence of the  $\delta/\pi$  versus  $\epsilon$  curves of two samples when  $\epsilon > 4.1\%$  suggests that different

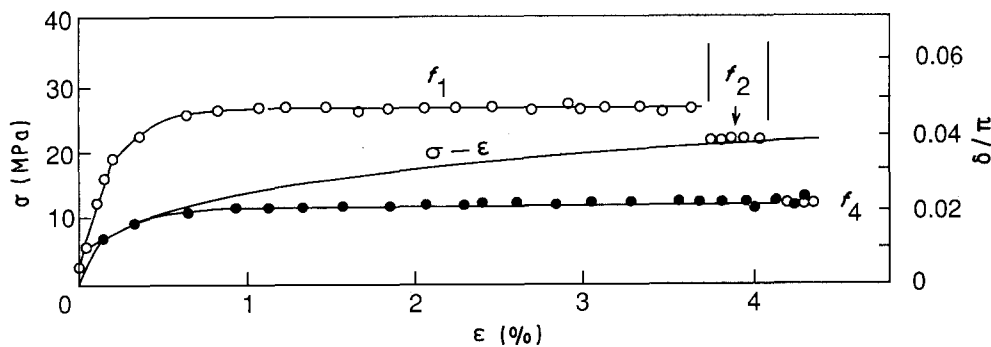


Figure 2 Effect of frequency on the  $\delta/\pi$  versus  $\epsilon$  curves at  $\dot{\epsilon} = 2.94 \times 10^{-6} \text{ s}^{-1}$  for  $f_1 = 0.386 \text{ Hz}$ ,  $f_2 = 0.5 \text{ Hz}$ ,  $f_4 = 1.0 \text{ Hz}$ . One sample (○) was tested at three frequencies,  $f_1$ ,  $f_2$  and  $f_4$ . The other sample (●) was tested at  $f_4$  only. The corresponding  $\sigma$  versus  $\epsilon$  curve is also shown.

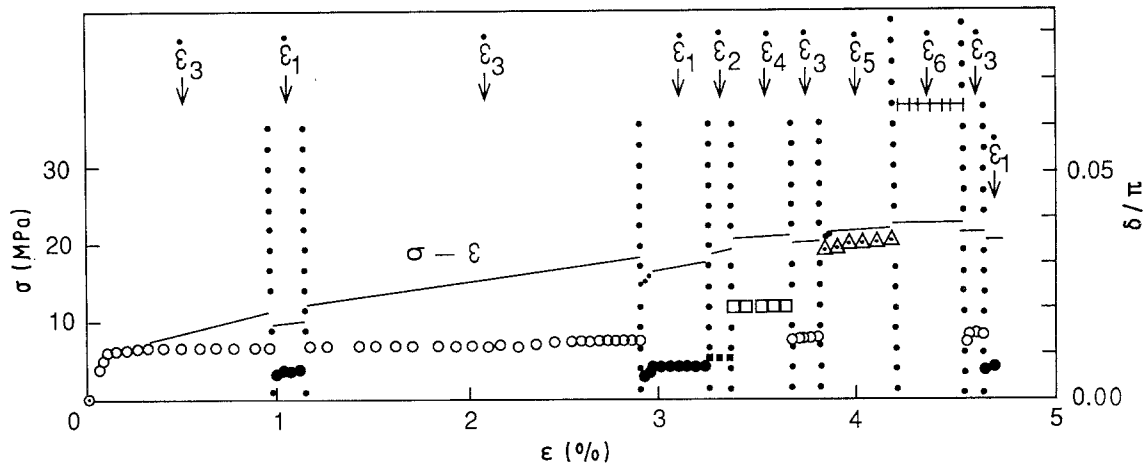


Figure 3 Effect of tensile strain rate,  $\dot{\epsilon}$ , on the  $\delta/\pi$  versus  $\epsilon$  data at constant  $f = 2.03$  Hz,  $\dot{\epsilon}_1 = 0.73 \times 10^{-6} \text{ s}^{-1}$ ,  $\dot{\epsilon}_2 = 1.53 \times 10^{-6} \text{ s}^{-1}$ ,  $\dot{\epsilon}_3 = 2.94 \times 10^{-6} \text{ s}^{-1}$ ,  $\dot{\epsilon}_4 = 6.35 \times 10^{-6} \text{ s}^{-1}$ ,  $\dot{\epsilon}_5 = 12.1 \times 10^{-6} \text{ s}^{-1}$ ,  $\dot{\epsilon}_6 = 25.3 \times 10^{-6} \text{ s}^{-1}$ . The corresponding  $\sigma$  versus  $\epsilon$  curves are also shown.

samples possess the same  $\delta/\pi$  value provided  $\dot{\epsilon}$ ,  $f$  and  $\epsilon$  are the same. It also implies that the reproducibility of internal friction measurement during plastic deformation is rather good and is unaffected by a change in the sample or in the frequency of vibration.

The effect of strain rate  $\dot{\epsilon}$  on the  $\delta/\pi$  versus  $\epsilon$  curve at constant frequency of measurement  $f_5 (= 2.03$  Hz) is shown in Fig. 3. The sample is stretched to  $\epsilon \sim 1\%$  with  $\dot{\epsilon}_3 = 2.94 \times 10^{-6} \text{ s}^{-1}$ , then to  $\epsilon \sim 1.2\%$  with  $\dot{\epsilon}_1 = 0.73 \times 10^{-6} \text{ s}^{-1}$ , to  $\epsilon \sim 2.85\%$  with  $\dot{\epsilon}_3$ , to  $\epsilon \sim 3.3\%$  with  $\dot{\epsilon}_1$ , and then to  $\epsilon \sim 4.7\%$  with  $\dot{\epsilon}_2 (= 1.53 \times 10^{-6} \text{ s}^{-1})$ ,  $\dot{\epsilon}_4 (= 6.35 \times 10^{-6} \text{ s}^{-1})$ ,  $\dot{\epsilon}_3$ ,  $\dot{\epsilon}_5 (= 12.1 \times 10^{-6} \text{ s}^{-1})$ ,  $\dot{\epsilon}_6 (= 25.3 \times 10^{-6} \text{ s}^{-1})$ ,  $\dot{\epsilon}_3$  and  $\dot{\epsilon}_1$ . As shown in Fig. 3,  $\delta/\pi$  increases with increasing  $\dot{\epsilon}$  and is almost parallel to the abscissa, especially at low strain rates.

In order to show the effect of  $\dot{\epsilon}$  and  $f$  more clearly, we transform the  $\delta/\pi$  values into  $Q^{-1}$  using Equation 3, and plot curves of  $Q^{-1}$  against  $\dot{\epsilon}$  at constant  $f$  (Fig. 4), and  $Q^{-1}$  against  $\omega^{-1}$  at constant  $\dot{\epsilon}$  (Fig. 5). Fig. 4 shows the non-linear effect of strain rate,  $\dot{\epsilon}$ , on  $Q^{-1}$  during plastic deformation at constant frequency of measurement. Fig. 5 shows the non-linear effect of frequency of measurement on  $Q^{-1}$  at constant strain rate. These figures show that, unlike the previously reported results [3–5],  $Q^{-1}$  exhibits a non-linear dependence on  $\dot{\epsilon}$  and on  $\omega^{-1}$ . The effect is more apparent at low frequencies and high strain rates.

Fig. 6 shows a plot of  $Q^{-1}$  against  $\dot{\epsilon}/\omega$  (all symbols in Fig. 6 coincide with those in Figs 4 and 5). The non-linear dependence of  $Q^{-1}$  on  $\dot{\epsilon}/\omega$  is apparent. The scatter of data in this figure compared with Figs 4 and 5 suggests that the dependences of  $Q^{-1}$  on  $\dot{\epsilon}$  and on  $\omega^{-1}$  are not the same. Even if  $\delta/\pi$  is used as an ordinate, the dependence of  $\delta/\pi$  on  $\dot{\epsilon}/\omega$  is still non-linear.

## 5. Discussion

### 5.1. Interrelationship between $Q^{-1}$ and $\epsilon$

It is well established that  $\dot{\epsilon} = \alpha \rho_m b v$ , where  $\alpha$  is an orientation factor,  $\rho_m$  is the density of mobile dislocations,  $b$  is the Burgers vector, and  $v$  is the average velocity of the dislocations. Since the strain rates con-

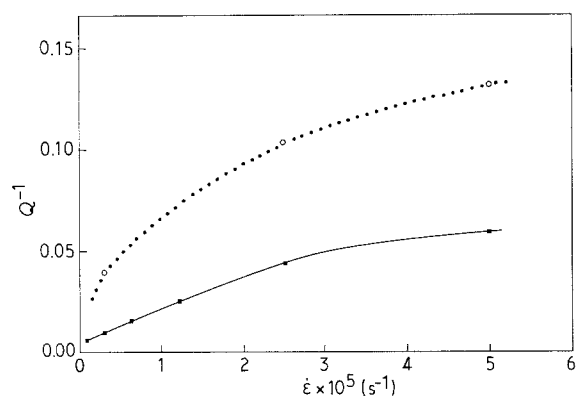


Figure 4 The non-linear dependence of  $Q^{-1}$  on  $\dot{\epsilon}$  for (O)  $f_1 = 0.382$  Hz and (■)  $f_5 = 2.03$  Hz;  $\epsilon = 3\%$ .

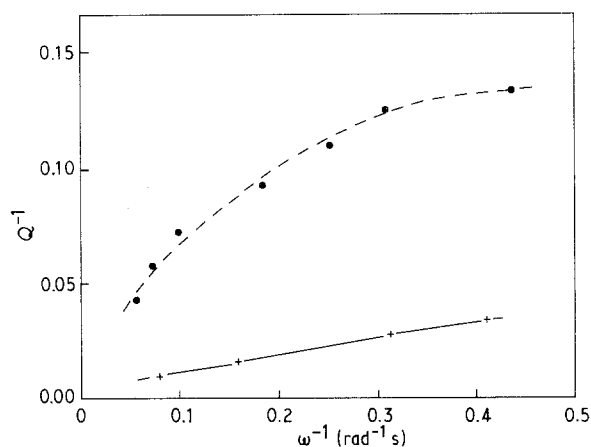


Figure 5 The non-linear dependence of  $Q^{-1}$  on  $\omega^{-1}$  for (●)  $\dot{\epsilon}_7 = 50 \times 10^{-6} \text{ s}^{-1}$  and (+)  $\dot{\epsilon}_3 = 2.94 \times 10^{-6} \text{ s}^{-1}$ ;  $\epsilon = 3\%$ .

sidered in this paper are low,  $\rho_m$  can be treated as independent of  $\dot{\epsilon}$  at a given value of strain. The dependence of  $Q^{-1}$  on  $\dot{\epsilon}$  is essentially a dependence of  $Q^{-1}$  on  $v$  at a given value of  $\epsilon$ . This implies that the study of internal friction during the process of plastic deformation can lead to an improved understanding of dislocation dynamics and strengthening mechanisms.

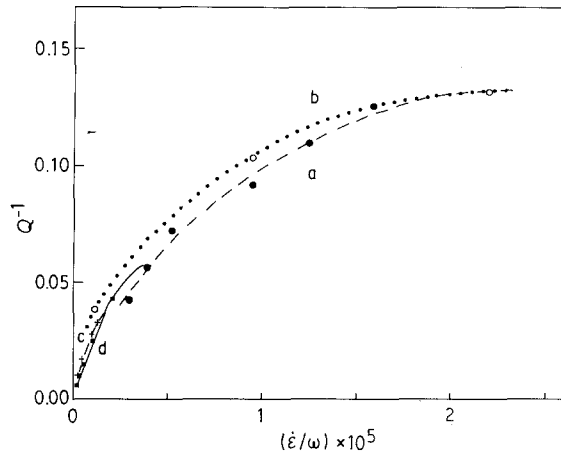


Figure 6 The non-linear dependence of  $Q^{-1}$  on  $\dot{\epsilon}/\omega$  (all symbols coincide with those in Figs 4 and 5). (a) Changing  $\omega$  at constant "high"  $\dot{\epsilon}$ , (b) changing  $\dot{\epsilon}$  at constant "low"  $\omega$ ; (c) changing  $\omega$  at constant "low"  $\dot{\epsilon}$ ; (d) changing  $\dot{\epsilon}$  at constant "high"  $\omega$ .  $\epsilon = 3\%$ .

## 5.2. Dependence of $Q^{-1}$ on $\omega$

The average velocity of mobile dislocations,  $v$ , is determined by the effective stress  $\sigma - \sigma_0$ , where  $\sigma_0$  is the back-stress dependent upon the density and distribution of various crystal defects. In this investigation,  $v$  has two components: a steady unidirectional component,  $v_0$ , and an alternating component,  $v_a$ , due to the oscillation of the pendulum. The former is essentially unaffected by the frequency of IF measurement. In order to obtain the correct dependence of  $Q^{-1}$  on  $\dot{\epsilon}$ , the influence of frequency will need to be separated from the effect of strain rate.

As shown in Fig. 6, the dependence of  $Q^{-1}$  on  $\dot{\epsilon}/\omega$  is different when the measurement is carried out at high frequency (curve d), and at low frequency (curve b). Thus, a complicated theoretical analysis is required to obtain the correct interrelationship between  $Q^{-1}$  and  $\dot{\epsilon}$ .

## 5.3. $Q^{-1}$ and dislocation dynamics

$Q^{-1}$  versus  $\epsilon$  and  $\sigma$  versus  $\epsilon$  curves can be measured simultaneously during plastic deformation. These curves can be converted into  $Q^{-1}$  versus  $\dot{\epsilon}$  and  $\sigma$  versus  $\dot{\epsilon}$  curves. The functional relationship between dislocation velocity and  $\sigma$  can be deduced from the dependence of  $Q^{-1}$  and  $\sigma$  on  $\dot{\epsilon}$ . This will be described in the following subsection.

## 5.4. Functional relationship between $v$ and $\sigma$

Consider a cylindrical specimen subjected to a tensile stress  $\sigma$  parallel to the longitudinal axis. The resolved shear stress  $\tau$  applied to the slip system is given by  $\tau = n_p \sigma$ , where  $n_p$  is an orientation factor. If the alternating resolved shear stress applied during internal friction measurement is  $\tau' = \tau'_0 \sin \omega t$ , where  $\tau'_0$  is a constant,  $\omega$  is the angular frequency and  $t$  is the time, then the total resolved shear stress applied to the slip system is  $\tau + \tau'$ . Since  $|\tau'| \ll \tau$ , we have  $v = f(\tau + \tau')$  and

$$v \simeq f(\tau) + \frac{df(\tau)}{d\tau} \tau' = v_0 + \frac{df(\tau)}{d\tau} \tau' \quad (4)$$

where  $v_0 = f(\tau)$  is the steady unidirectional component of  $v$  parallel to the slip direction (see section 5.2).

The vibrational energy per unit volume dissipated per cycle by the mobile dislocations is given by

$$\begin{aligned} \Delta W &= \rho_m \int_0^T b \tau' v dt \\ &= \rho_m b \int_0^T \tau' \left( v_0 + \frac{df(\tau)}{d\tau} \tau' \right) dt \\ &\simeq \rho_m b \frac{df(\tau)}{d\tau} \int_0^T (\tau'_0)^2 \sin^2 \omega t dt \\ &= \left( \frac{df(\tau)}{d\tau} / f(\tau) \right) \frac{\pi \dot{\gamma}}{\omega} (\tau'_0)^2 \\ &= \frac{d \ln f(\tau)}{d\tau} \left( \frac{\pi \dot{\gamma}}{\omega} \right) (\tau'_0)^2 \end{aligned}$$

where  $\dot{\gamma} = b \rho_m v_0$  is the plastic shear strain rate. Let the stress amplitude used in internal friction measurement be  $\tau'_0$ . For longitudinal vibration, the resolved shear stress amplitude  $\tau'_0$  equals  $n_p \tau'_0$ . The total vibration energy per unit volume may be written as  $W = (\tau'_0)^2 / 2E = (\tau'_0)^2 / 2\bar{n}_p^2 E$ , where  $\bar{n}_p$  is an average orientation factor and  $E$  is the Young's modulus.

For torsional vibration, the resolved shear stress is  $\tau'_0 = n_t \tau'_0$ , where  $n_t$  is the orientation factor for torsional stress. The total vibration energy per unit volume is  $W = (\tau'_0)^2 / 2\bar{n}_t^2 G$ , where  $\bar{n}_t$  is the average orientation factor and  $G$  is the shear modulus.

Thus, for longitudinal vibrations the internal friction during the process of plastic deformation is

$$Q^{-1} = \frac{d \ln f(\tau)}{d\tau} \bar{n}_p \frac{E \dot{\epsilon}}{\omega} \quad (5)$$

For torsional vibrations, the internal friction during plastic deformation is

$$\begin{aligned} Q^{-1} &= \frac{d \ln f(\tau)}{d\tau} \left( \frac{\bar{n}_t^2}{\bar{n}_p} \right) \frac{G \dot{\epsilon}}{\omega} \\ &= \frac{d \ln f(\sigma)}{d\sigma} \left( \frac{\bar{n}_t^2}{\bar{n}_p^2} \right) \frac{G \dot{\epsilon}}{\omega} \quad (6) \end{aligned}$$

For b.c.c. metals,  $\bar{n}_t^2 / \bar{n}_p \simeq 0.223$  and  $\bar{n}_t^2 / \bar{n}_p^2 \simeq 0.5$ ; for f.c.c. metals,  $\bar{n}_t^2 / \bar{n}_p \simeq 0.274$  and  $\bar{n}_t^2 / \bar{n}_p^2 \simeq 0.85$  [5]. Thus

$$Q^{-1} = 0.85 \frac{d \ln f(\tau)}{d\tau} G \frac{\dot{\epsilon}}{\omega} \quad (7)$$

If the Johnston-Gilman equation [8],  $v = f(\sigma) = B'(\tau - \tau_0)^m = B(\sigma - \sigma_0)^m$ , is applied, we have

$$Q^{-1} = \frac{0.85 m G}{\sigma - \sigma_0} \left( \frac{\dot{\epsilon}}{\omega} \right) \quad (8)$$

If the other equation,  $v = v^* \exp[-\sigma^*/(\sigma - \sigma_0)]$ , suggested by Gilman [9] and Zhang [7] is applied, then

$$Q^{-1} = \frac{0.85 \sigma^* G}{(\sigma - \sigma_0)^2} \left( \frac{\dot{\epsilon}}{\omega} \right) \quad (9)$$

where  $v^*$  is a characteristic velocity ( $\lesssim$  velocity of transverse sound wave) and  $\sigma^*$  is a characteristic dragging force when  $v = v^*/e$ .

The dependence of  $Q^{-1}$  on  $\dot{\epsilon}/\omega$  in Equations 7 to 9 is non-linear because the effective stress ( $\sigma - \sigma_0$ ) depends on  $\dot{\epsilon}$ . Different dislocation dynamics equations give different expressions for  $Q^{-1}$ . What we have shown is that the non-linear dependence of  $Q^{-1}$  on tensile strain rate and frequency can be explained on the basis of dislocation dynamics.

## References

1. R. E. MARINGER, *J. Appl. Phys.* **24** (1953) 1525.
2. T. S. KÈ, P. T. YANG and C. C. CHANG, *Sci. Rec.* **1** (1957) 231.
3. V. S. POSTNIKOV, Yu M. EL'KIN and S. I. MESHKOV, *Sov. Phys. Solid State* **8** (1967) 2919.
4. P. FELTHAN and C. R. NEWHAN, *J. Mater. Sci.* **4** (1969) 170.
5. J. X. ZHANG, G. L. OU and Y. X. HU, *Acta Phys. Sinica* **29** (1980) 354.
6. T. S. KÈ and J. X. ZHANG, *ibid.* **24** (1975) 817.
7. J. X. ZHANG, *J. Physique* **42** (1981) C5-399.
8. W. G. JOHNSTON and J. J. GILMAN, *J. Appl. Phys.* **29** (1959) 877.
9. J. J. GILMAN, *ibid* **36** (1965) 727.

*Received 28 October 1991  
and accepted 14 August 1992*